Properties of iron impurities in beryllium from Mössbauer studies

C. Janot, P. Delcroix, and M. Piecuch
Laboratoire de Physique du Solide, Université de Nancey-I-C. O. 140, 54037 Nancy-Cedex, France
(Received 7 August 1972; revised manuscript received 15 April 1974)

Beryllium specimens containing 0.012-at. % ^{57}Fe were studied by Mössbauer spectroscopy in the temperature range from 75 to 1200 K. The changes of the recoil-free fraction, the second-order Döppler shift, the isomer shift, the quadrupole splitting, and the peak intensities are reported and interpreted as follows. (i) The effective impurity-host force constant λ' is slightly smaller than the host-host force constant λ ($\lambda'/\lambda \sim 0.96$) and an anharmonic behavior is observed at high temperature. (ii) The main part of the electric field gradient arises from *d* electrons localized around the impurity atom in a virtual bound state near the Fermi level. (iii) At about 870 K, a short-range diffusion process occurs for iron impurities in as-quenched specimens with progressive annealing of quenched defects.

INTRODUCTION

Mössbauer data have provided an important contribution to a better understanding of the nature and the properties of defects in crystalline solids,[1] especially with respect to the electronic and dynamical properties of chemical impurities in metals.

Among other Mössbauer results, the nuclear quadrupole interaction in hexagonal close-packed metals has been the subject of great interest in recent years, though the exact origin of the electric field gradient (EFG) is still not well understood.

For instance, the sign of the EFG on iron is found to be negative in Be[2] and positive in zinc,[3,4] whereas precise methods of calculation[5,6] and NMR experiments[7] give just the opposite signs for the EFG on the host atoms. A possible explanation of this discrepancy seems to lie in a large contribution to the EFG from the nonspherical distribution of electrons within the atomic sphere surrounding the iron impurity.[8–10] The present work gives some experimental evidence for the existence of localized electronic states which have a nonspherical distribution around the impurities and which obviously contribute to the EFG.

Another important problem concerning chemical impurities in quenched metals is to obtain information on the clustering process of quenched vacancies and dislocation loop nucleation, in particular about the impurity atom. The recoilless fraction in combination with the hyperfine splitting of the Mössbauer radiation from impurities in a host lattice is a unique sensor of the local interatomic potential and the spatial symmetry of the immediate surroundings of the impurity sites; so, Mössbauer studies can complement the investigations made by x-ray topography[11] and electron microscopy.[12]

SPECIMEN PREPARATION AND EXPERIMENTAL PROCEDURE

The beryllium host element used was of the highest commercially available purity and contained about 300-ppm residual impurities. Iron was enriched with ^{57}Fe. The samples were prepared by the standard arc melting technique, homogenized by repeated melting, annealed at 1200 °C for a week, and finally quenched in brine.[13] The effective thickness of the samples observed in Mössbauer spectroscopy was 0.6 μm in ^{57}Fe (or 10^{19} atoms of ^{57}Fe/cm^2).

The Mössbauer experiments were done with a spectrometer operating in the constant acceleration mode. The 25-mCi source used was prepared by electroplating ^{57}Co* onto palladium and then reducing and diffusing in H_2 atmosphere at high temperature. The velocity scale and the spectral-shift origin have been normalized to a natural iron absorber whose peak half-width is 0.119 mm/sec. The peak positions are determined with an accuracy of better than 0.002 mm/sec and their relative intensities can be evaluated with an error of a few percent. Ten *Be*-Fe samples were studied in such a way.

The spectra were obtained at various temperatures with the use of a cryostat and a vertical vacuum furnace provided with some windows transparent to γ rays (beryllium or Mylar). In both systems, the temperature remains stable with an accuracy of approximately 0.1%. Each raw spectrum for the iron impurity is a typical quadrupole split doublet as shown in Fig. 1. A numerical computer analysis yields the following useful parameters: the position and relative intensity of each peak, and the half-width Γ of each peak.

From these data, it is possible to deduce (i) the total shift δ of the spectrum (isomer shift plus second-order Doppler shift) and the quadrupole splitting ΔE_Q, both expressed in mm/sec; the reproducibility of the results among the ten specimens is better than ± 0.002 mm/sec for the total shift and ± 0.004 mm/sec for the quadrupole splitting; (ii) the ratio I_1/I_2 of peak intensities (the subscript 1 refers to the peak of lower energy), for which

the reproducibility among the ten specimens observed is about 5%; (iii) the recoil-free fraction f, obtained by supposing a proportionality law between f and the area of the spectra for samples having the same effective thickness. The reference is the value $f = 0.80$ at room temperature.[14] The reproducibility among the samples is here about 10%.

In this study, the behavior of these parameters (δ, ΔE_Q, I_1/I_2, and f) is studied on each as-quenched sample during a first measurement sequence from 75 to 1200 K; since some annealing takes place during these measurements, the data are called "partially annealed" when the above measurements are repeated on each sample in a second sequence.

RESULTS

Typical spectra shown in Fig. 2 clearly indicate significant changes in the shift and the splitting, as well as in the relative intensities of the two peaks. Tables I and II give the mean numerical data obtained from the different Mössbauer observations (Table I corresponds to the mean data taken on as-quenched samples and Table II to the mean data taken on partially annealed samples as stated above).

The data in Figs. 3, 4, 5, and 6 show, respectively, the variations of $\ln(f(T))$, $(I_1/I_2)(T)$, $\delta(T)$, and $\Delta E_Q(T)$. All of these results lead to the following remarks.

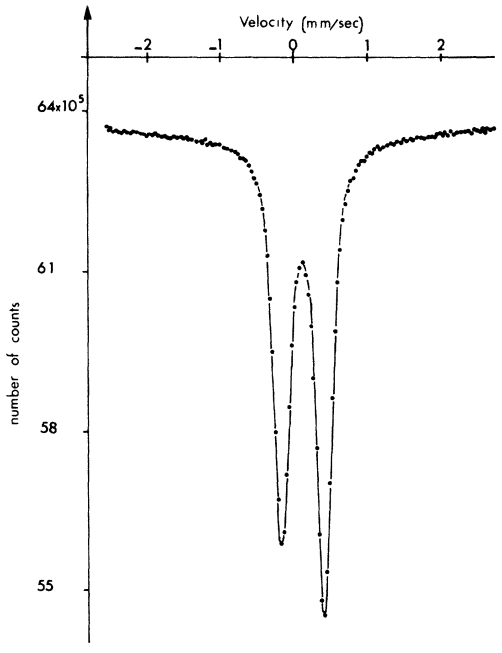

FIG. 1. Typical Mössbauer spectrum obtained at room temperature for a beryllium based alloy containing 0.012-at.% ^{57}Fe.

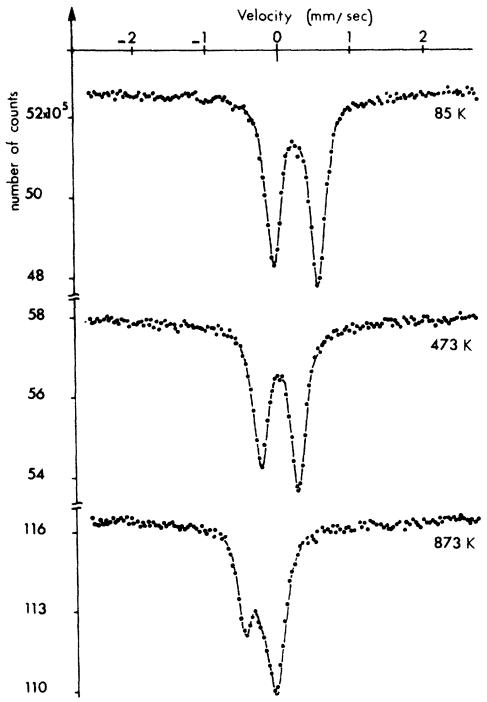

FIG. 2. Changes in the spectrum as a function of the observation temperature (85, 473, 873 K).

(i) The data on $\ln(f(T))$, $\delta(T)$, and $\Delta E_Q(T)$ are practically the same in the two-measurement sequences (as-quenched and then partially annealed samples). They vary smoothly with the temperature.

(ii) The curve of Fig. 4 shows an important drop of the ratio I_1/I_2 near 870 K, especially in the case of as-quenched specimens. This drop does not completely vanish when the alloys are partially annealed, but it decreases significantly.

(iii) The Debye-Waller factor $2W = -\ln f$ varies linearly from about 300 to 750 K, but Fig. 3 indicates the appearance of an anharmonic contribution to the mean-square displacement of the atoms as soon as the temperature reaches about 900 K.

(iv) If the total shift $\delta(T)$ of the spectra depended on the temperature only as the second-order Doppler effect, we should obtain a variation law $-3kT/2mc = -7.3\times10^{-4}\,T$ mm/sec[15] when the temperature is high enough, thus making the classical approximation valid. The experimental data give, rather, $-(7.8\pm0.1)\times10^{-4}\,T$ mm/sec, for a temperature range from 450 to 950 K. This significant difference is consistent with a decrease of the isomer shift $\delta_{iso}(T) = \delta_{iso}(0) - (0.5\pm0.1)\times10^{-4}T$. The high-temperature straight line intersects the ordinate axis at the value +0.376 mm/sec. Since the extrapolated experimental value $\delta(0)$ is 0.250 mm/sec, we can obtain the second-order Doppler effect at 0 K:

TABLE I. Evolution of Mössbauer parameters for an as-quenched specimen.

T (K)	δ (mm/sec)/Fe	ΔE_Q (mm/sec)	I_1/I_2	ln$f$
4	...	−0.63 (Ref. 29)	...	...
80	+0.232	−0.625	0.85	−0.20
113	+0.227	−0.622	0.85	−0.20
153	+0.207	−0.618	0.85	−0.20
193	+0.186	−0.610	0.84	−0.22
233	+0.164	−0.601	0.82	−0.22
273	+0.140	−0.585	0.81	−0.22
298	+0.118	−0.571	0.82	−0.23
333	+0.095	−0.560	0.82	−0.23
373	+0.051	−0.543	0.84	−0.24
423	+0.035	−0.526	0.82	−0.27
473	−0.034	−0.514	0.82	−0.34
523	−0.038	−0.500	0.83	−0.35
573	−0.073	−0.487	0.83	−0.38
623	−0.109	−0.472	0.85	−0.43
673	−0.149	−0.452	0.83	−0.47
723	−0.183	−0.443	0.80	−0.53
773	−0.221	−0.425	0.83	−0.60
823	−0.244	−0.391	0.55	−0.49
873	−0.278	−0.379	0.54	−0.58
923	−0.328	−0.371	0.56	−0.58
973	−0.368	−0.370	0.77	−0.75
1023	−0.412	−0.352	0.78	−0.85
1073	−0.447	−0.340	0.80	−0.97

$$\Delta S(0) = 0.376 - 0.250 = 0.126 \pm 0.004 \text{ mm/sec} .$$

(v) While heating the specimen the absolute value of the quadrupole splitting clearly decreases; the slope of ΔE_Q vs T seems to be larger at high temperature than at low temperature. These experimental data show much contrast with what could be expected from the anisotropic thermal expansion. Indeed, if only the latter was responsible for the changes in quadrupole splitting, according to Refs. 6 and 8 we should have

$$\Delta E_Q = (K_1/a^3)[0.0065 - 4.3584\,(c/a - 1.633)] , \quad (1)$$

where a and c are the lattice parameters and K_1 is a constant factor (obtained by fitting ΔE_Q with an experimental value at room temperature, for instance). Then, from $a_0 = 2.286$ Å, $c_0 = 3.584$ Å[16] at room temperature, and from the linear coefficients of thermal expansion in beryllium, a certain value of ΔE_Q could be calculated for each temperature leading to a type of variation as shown by the dashed curve of Fig. 6. Let us note that the shape of this dashed curve is well defined by Eq. (1); but its position depends on the factor K_1 which cannot be estimated theoretically if the electronic structure of the iron impurity is unknown.

INTERPRETATION AND DISCUSSION

The experimental results give rise to two types of observations for which the following distinct explanations are proposed: (i) an over-all evolution of the Mössbauer parameters ($\delta, f, \Delta E_Q$) in direct connection with the dynamical and electronic properties of the isolated iron impurity in beryllium; and (ii) an adventitious evolution of I_1/I_2 near 870 K called an "anomaly," mainly observed for an as-quenched sample, of a more metallurgical origin, connected to some modification in the impurity neighborhood.

A. Dynamical properties of the iron impurity

The recoilless fraction and the second-order Doppler shift can be expressed, respectively, as a function of the mean-square displacement and the mean-square velocity of the resonant atom. We can obtain a good description[15] of $\langle x^2 \rangle$ and $\langle v^2 \rangle$ for the impurity atoms with the use of the Debye model corrected by an effective Debye temperature Φ_D:

$$\Phi_D = \Theta_D (m/m')^{1/2} (\lambda'/\lambda)^{1/2} , \quad (2)$$

where Θ_D is the Debye temperature for the pure host metal, m is the mass of the host atoms, λ is the force constant in the host metal, and m' and λ' are the same quantities corresponding to the iron impurities. According to this model,[15,19,35] we can obtain the resonant recoilless fraction and the second-order Döppler effect from the relations

TABLE II. Mössbauer parameters for a partially annealed specimen, first with temperature increasing, then decreasing.

T (K)	δ (mm/sec)/Fe	ΔE_Q (mm/sec)	I_1/I_2	ln$f$
80	+0.237	−0.609	0.87	−0.14
113	+0.227	−0.607	0.87	−0.14
153	+0.212	−0.601	0.87	−0.14
193	+0.190	−0.591	0.88	−0.15
233	+0.163	−0.585	0.86	−0.15
273	+0.138	−0.572	0.87	−0.18
298	+0.119	−0.566	0.87	−0.21
333	+0.091	−0.553	0.86	−0.27
373	+0.051	−0.537	0.88	−0.30
423	+0.030	−0.529	0.83	−0.30
473	−0.006	−0.512	0.80	−0.34
523	−0.032	−0.498	0.82	−0.39
573	−0.077	−0.485	0.83	−0.42
623	−0.112	−0.469	0.82	−0.47
673	−0.150	−0.458	0.79	−0.50
723	−0.179	−0.443	0.81	−0.50
773	−0.221	−0.432	0.81	−0.58
823	−0.251	−0.412	0.75	−0.59
873	−0.290	−0.398	0.70	−0.62
923	−0.349	−0.386	0.67	−0.67
973	−0.371	−0.378	0.74	−0.83
1023	−0.428	−0.367	0.76	−0.86
1073	0.463	−0.342	0.85	−0.95
1123	−0.503	−0.322	0.85	−0.95
1073	−0.464	−0.348	0.81	−0.95
873	−0.332	−0.398	0.80	−0.63
473	−0.039	−0.522	0.82	−0.35

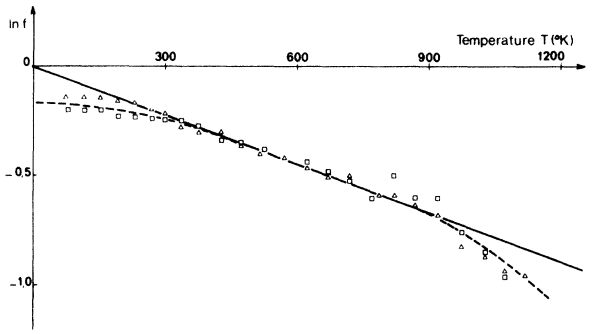

FIG. 3. Debye-Waller factor $2W = -\ln f$ vs temperature: □, as-quenched specimen; △, partially annealed specimen; solid line (——), high-temperature linear variation.

$$f = \exp\left\{-\frac{3E_0^2}{4m'c^2k\Phi_D}\left[1+4\left(\frac{T}{\Phi_D}\right)^2\int_0^{\Phi_D/T}\frac{y\,dy}{e^y-1}\right]\right\}, \tag{3}$$

$$\Delta S = \frac{9k\Phi_D}{16m'c}\left[1+8\left(\frac{T}{\Phi_D}\right)^4\int_0^{\Phi_D/T}\frac{y^3\,dy}{e^y-1}\right]. \tag{4}$$

The Debye-integral functions which appear in these expressions are tabulated[17] and can be easily used; E_0 is the energy of the Mössbauer transition. From (4), the second-order Doppler shift can be expressed at $T = 0$ K:

$$\Delta S(0) = 9k\Phi_D/16m'c\ . \tag{5}$$

As the experimental value of $\Delta S(0)$ is 0.126 ± 0.004 mm/sec, we can obtain the effective Debye temperature

$$\Phi_D^0 = 452 \pm 18\ \text{K},$$

and relation (2) leads to $\lambda'/\lambda \simeq 0.96 \pm 0.05$ by using the value $\Theta_D = 1160$ K for pure beryllium at 0 K.[18] This result is in good agreement with that proposed by Schiffer *et al.*[19]

In the same way, relation (4) gives the recoilless fraction at high temperature

$$\ln f_{HT} = -(3E_0^2/m'ck\Phi_D^2)\,T\ . \tag{6}$$

As Fig. 3 shows roughly a straight line for $\ln(f(T))$ from 450 to 950 K, we can still deduce Φ_D from the comparison between (6) and the slope of this curve; so, we find

$$\Phi_D^{HT} = 415 \pm 21\ \text{K}.$$

This result is consistent with the value $\Theta_D^{HT} = 1062$ K (Ref. 18), $\lambda'/\lambda \simeq 0.96 \pm 0.05$, and relation (2).

We note (Fig. 3) that f moves away from its regular variation when the temperature reaches about 950 K. This rapid decrease of the recoilless fraction can be explained by the anharmonic character of the atomic vibrations, which become big enough

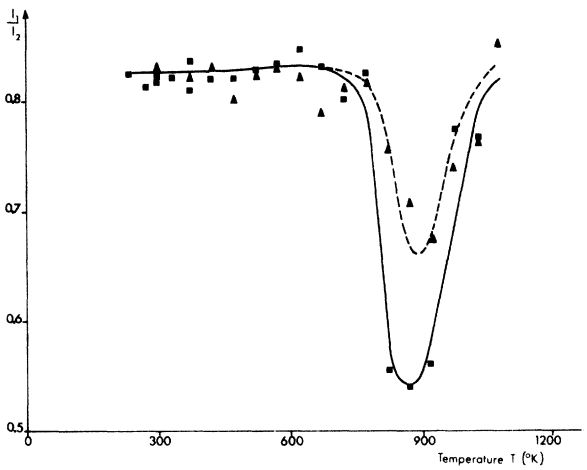

FIG. 4. Ratio of the peak intensities vs temperature $(I_1/I_2)(T)$: ■, as-quenched specimen; ▲, partially annealed specimen.

to influence the behavior of $\langle x^2\rangle$. These anharmonic effects manifest themselves in the form of changes in vibration frequencies as a function of temperature.[15,20] A large contribution to the effects arises from the lattice thermal expansion, and as a first approximation, we use in general the "quasiharmonic" model, which takes only this contribution into account. In a perfect crystal, the changes of the atomic-vibration frequencies ω_i can be connected to the volume through the Grüneisen constant

$$\gamma = -\frac{\partial \log\omega_i}{\partial \log V} = -\frac{1}{\omega_i}\frac{\partial\omega_i}{\partial T}\Big/\frac{1}{V}\frac{\partial V}{\partial T}.$$

Introducing the volume coefficient of thermal expansion $\beta = (1/V)(\partial V/\partial T)$ gives

$$\gamma = \frac{1}{\beta\omega_i}\frac{\partial\omega_i}{\partial T}$$

and

$$\omega_i(T) = \omega_i^0 \exp\left(-\gamma\int_0^T \beta(T')\,dT'\right),$$

where ω_i^0 is the vibration frequency of the mode i at $T = 0$ K and γ is assumed to vary slowly with temperature. This leads, in particular, to a variation of the Debye temperature

$$\Theta_D(T) = \Theta_D^0 \exp\left(-\gamma\int_0^T \beta(T')\,dT'\right) \tag{7}$$

and then to the Debye-Waller factor in the high-temperature limit which can be written from relations (6) and (7):

$$2W = -\ln f = \frac{3E_0^2}{mc^2}\frac{T}{k(\Theta_D^0)^2}\exp\left(2\gamma\int_0^T \beta(T')\,dT'\right)$$

$$\simeq \frac{3E_0^2}{mc^2k(\Theta_D^0)^2}\, T(1+\epsilon T) ,$$

where

$$\epsilon = \frac{2\gamma}{T}\int_0^T \beta(T')\,dT' = 2\gamma\bar{\beta} .$$

Assuming the result valid as a first approximation for the iron impurity in a beryllium matrix, we should have

$$2W' = (3E_0^2/m'c^2k\Phi_D^2)\, T(1+\epsilon' T) ,$$

where Φ_D has the previously given value at high temperature (415 K) and W' is the Debye-Waller factor for the iron impurity.

The anharmonic coefficient ϵ in pure beryllium can be calculated from $\gamma \sim 1.15$ and β (Ref. 18); this leads to $\epsilon \simeq (1 \pm 0.1)\times 10^{-4}$. The anharmonic coefficient ϵ' around the iron impurity can be obtained from the deviation between the measured Debye-Waller coefficient (dashed curve in Fig. 3) and the expected one (Debye straight line in Fig. 3); this leads to $\bar{\epsilon}' \simeq (1.5 \pm 0.2)\times 10^{-4}$, with a slow increase of ϵ' when the temperature rises ($\epsilon' \simeq 1.4 \times 10^{-4}$ at 900 K and $\epsilon' \simeq 1.7\times 10^{-4}$ at 1200 K).

Therefore, the deviation from Debye's model seems to be sufficiently explained by the anharmonicity; Table III shows that the difference between $\bar{\epsilon}'$ and ϵ found here can be reasonably fitted into the range of experimental values obtained elsewhere[15,21] for other metals containing iron as an impurity.

However, as discussed later, if the behavior of $(I_1/I_2)(T)$ appearing in the spectra near 870 K was connected to a sort of phase change, that could explain in another way why $\langle x^2 \rangle$ does not strictly follow a Debye law.

TABLE III. Anharmonic coefficients for iron impurity in various metals.

Matrix	γ	$\epsilon(10^{-4})$	$\epsilon'(10^{-4})$	Θ_D	Φ_D
Ir	2.75	1.17	0.92	285	457
Rh	2.26	1.46	0.67	350	427
Pt	2.54	1.38	0.97	233	363
Pd	2.23	1.55	6.14	275	373
Au	3.0	2.54	7	164	329
Cu	2.0	2.07	6.85	343	397
Al	3.3	4.5	2.8	418	250
Be	1.15	1.0	1.5	1062	415

B. Electronic properties of the iron impurity

Other important information can be obtained from the changes of the quadrupole splitting which, as previously stated, cannot be explained neither by the hexagonal structure of the host metal nor by the anisotropic expansion with temperature.

In hexagonal close-packed metal three important contributions to the EFG eq are commonly recognized. The first is the direct lattice field gradient $eq^{\rm lat}$ which arises from the incompletely screened positive-ion core of the lattice. A second contribution $eq^{\rm elec}$ is believed to arise from the nonspherical distribution of electrons within the atomic sphere surrounding a particular nuclear site. And the third contribution arises from the closed shells which become distorted under the influence of the nonspherical potential associated with $eq^{\rm lat}$ and $eq^{\rm elec}$. This third contribution is generally ex-

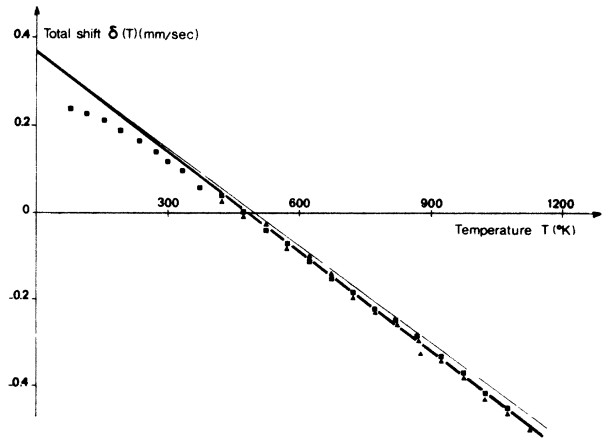

FIG. 5. Total displacement of the spectrum (isomer shift plus second-order Döppler effect) vs the temperature: solid line (—) straight line with a slope $3k/2m'c$; solid line (—) high-temperature experimental straight line; ■, as-quenched specimen; ▲, partially annealed specimen.

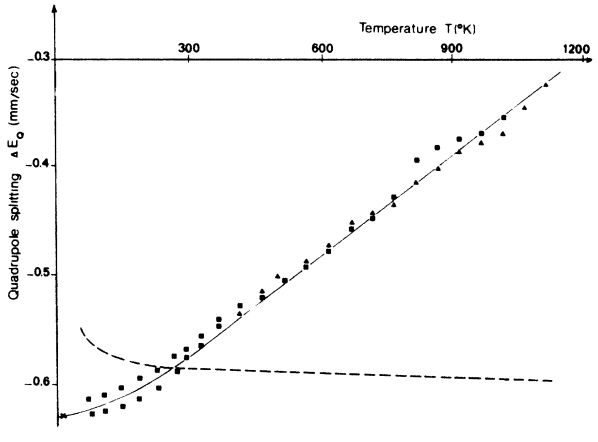

FIG. 6. Quadrupole splitting as a function of the temperature. The dashed curve gives what could be changes in the quadrupole splitting if only the anisotropic thermal expansion was taken into account. The thin solid line is a fit of the data using Eq. (8) where n_{dF} is assumed to be linear in T. ■, as-quenched specimen; ▲, partially annealed specimen; ×, from Ref. 29.

pressed in terms of Sternheimer antishielding and shielding factors γ_∞ and R_Q, respectively. Thus,

$$eq = (1-\gamma_\infty)\, eq^{\mathrm{lat}} + (1-R_Q)\, eq^{\mathrm{elec}} .$$

As reported above, the evaluation of eq^{lat} is possible by considering the crystal as an electrostatic assembly of point charges (the ion cores) which are embedded in a uniform sea of negative charges (the conduction electrons). We have used the results of such a model[16] and a more highly perfected one[5]; it gives a positive or negative contribution to the quadrupole splitting for hcp metals depending on the ratio c/a, as shown from relation (1). In the case of beryllium, we shall have from (1)

$$\Delta E_Q^{\mathrm{lat}} \simeq (1-\gamma_\infty)0.0132 \text{ mm/sec}$$

$[(1-\gamma_\infty)0.0131$ if $T = 75$ K and $(1-\gamma_\infty)0.00133$ if $T = 800$ K].

According to the work of Watson *et al.*,[8] the contribution arising from the nonspherical distribution of conduction electrons within the atomic sphere is proportional to the lattice field gradient and has the opposite sign. In fact, this result is obvious since the conduction electrons have a negative electric charge (compared with the positive ions) and are distributed with respect to the hexagonal structure of the ions.

In such a model, the quadrupole splitting of the ion impurity in beryllium should be given again by an expression like (1), with a new K_1 factor depending on the proportionality between lattice and electronic field gradients as well as on the Sternheimer factors. As previously stated, the changes of the quadrupole splitting with the temperature due to anisotropic expansion would be as shown by the dashed curve in Fig. 6. While the experimental absolute value of the quadrupole splitting decreases by about 46%, the dashed curve increases by only a few percent.

So, it is obvious that we need to invoke a rather important modification in the electronic content of the iron atomic sphere when the beryllium is heated.

A possible reduction of the nonspherical distribution of conduction electrons within the atomic sphere by an s-p exchange process[22] is no longer a good explanation since it cannot be larger than a few percent, as shown by experimental results regarding the Knight-shift behavior in NMR.[23,24]

An explanation seems to lie in the existence of degenerate virtual bound $3d$ states on the iron impurities, just below the Fermi level of the s-p conduction band. Indeed, when an impurity of higher charge is substituted for an atom of a host metal, the well-known Friedel-Anderson[25] theory shows that a number of outer electrons of the impurity, corresponding to those shells whose energies lie within the host-metal conduction band, are delocalized and go off into the conduction band. Consequently, this will result in both an excess of positive charges at the impurity and vacant electronic states at energy E_d. When a conduction electron approaches the impurity site with an energy near E_d, it will be caught and resonantly scattered before going off once again. As a result of this scattering process, negative charges accumulate in the vicinity of the impurity and locally screen the impurity potential; it can be shown that charge oscillations occur around the impurity[25] and that the density of d states at the Fermi level $n_d(\epsilon_F)$ depends on the amplitude of these charge oscillations.[26] Then, if the virtual bound states are just below the Fermi level, $n_d(\epsilon_F)$ will depend on the temperature. According to Watson *et al.*,[8] the electronic contribution on the EFG should be linearly related to $n_d(\epsilon_F)$, so the decrease in the absolute value of the quadrupole splitting on Fe in Be could be explained. Let us notice that the assumptions of Watson *et al.* are strongly supported by the works of Window and Longworth[27] which shows that the EFG and residual resistivity at room temperature change in the same way among various alloys with iron impurities. On the other hand, macroscopic studies on dilute alloys of Ni in Be (Ref. 28) show that virtual bound $3d$ states can be expected on transition impurities (such as iron) in normal hcp host metals (such as beryllium). The degenerate character of these $3d$ states is suggested by the magnetic behavior of the material, which indicates that there is no magnetic moment on the iron impurity.[29]

In the expression of the quadrupole splitting on Fe in Be, the effect of anisotropic thermal expansion should therefore be modulated by a temperature-dependent term like the density of $3d$ states at the Fermi level $n_{dF}(T)$:

$$\Delta E_Q(T) = (K_2/a^3)[0.0065 - 4.3584\,(c/a - 1.633)] \times n_{dF}(T) . \quad (8)$$

It is clear from Fig. 6 that a linear fit of $\Delta E_Q(T)$ is not too bad, especially when the temperature is higher than 300 K:

$$(K_2/a^3) n_{dF}(T) \simeq 0.66(1 - T/2190) . \quad (9)$$

This result is consistent with the temperature dependence of the amplitude of the charge oscillation around $3d$ transition-metal impurities in normal metals measured by the NMR method,[26] or residual resistivity determined as a function of the temperature.[30] Indeed, both of them, well known to be linear in n_{dF}, experimentally show a linear temperature dependence.

C. Annealing of the quenched defects

Let us consider the "anomaly" in the spectra

which starts at 775 K, takes its highest value at 870 K, and vanishes at 975 K, especially during the first measurement sequence on an as-quenched sample. The phenomenon appears to a lesser degree during the second measurement sequence (see Fig. 4) being visible on the curve $(I_1/I_2)(T)$, and then it completely disappears after three measurement sequences.

It should be pointed out that the anomalous effects cannot be due to a gradual pickup of impurities from the atmosphere in the furnace during measurements, although beryllium is highly sensitive to contamination. It is difficult to obtain a vacuum better than 10^{-6} Torr in a furnace provided with optical windows and at a temperature of 1200 K, but the anomalous phenomenon does not grow and even progressively disappears by successive heating sequences of one sample. A gradual contamination by interstitials would certainly produce an opposite effect.

Usually, if the ratio of quadrupole line intensities is not unity with a polycrystalline specimen, either the alloys exhibit a crystalline texture or anisotropy occurs in the mean-square displacement of the iron atoms. The former can be excluded because there are few possibilities for new crystalline texture to appear during the measurement sequences for the following reasons: (i) At the end of the preparation, the specimens have been annealed at 1200 °C for a week; a possible large-grain growth process would have appeared during this time; in fact, it did, since the ratio I_1/I_2 always deviated significantly from unity, even outside of the anomaly range ($I_1/I_2 \simeq 0.85 \pm 0.03$). (ii) It would be difficult to explain the appearance of a texture at 900 K and then its disappearance at 1000 K with an as-quenched sample, and why this texture would reappear to a lesser degree during the second measurement sequence and then would not reappear at all after three measurement sequences.

As for the assumed anisotropy in the mean-square displacement of the iron atoms, it is clear that the observed effect is too strong to correspond to a vibrational anisotropy[31]; but a short-range anisotropic diffusion process could occur. As a matter of fact, metallurgical studies[32–34] have shown that iron diffuses in beryllium as soon as the temperature reaches about 800 K and that quenched defects in beryllium segregate to form small dislocation loops on the basal plane, especially around impurities. These considerations suggest that a short-range diffusion process of iron in the basal plane could occur from about 800 K to nearly 900 K, with iron atoms jumping from one site of a loop to another. As the temperature reached a high-enough value (about 900 K), the loops would be progressively annealed and consequently the process would disappear. As experimentally verified,[11] the complete annealing of such quenched defects in metal often requires several heating sequences; the same had to be done in the present work for I_1/I_2 to remain constant over the whole temperature range.

During the process of short-range diffusion, the recoilless fraction would almost vanish except for the grains which are oriented in such a way that the iron displacement occurs perpendicularly to the emitted γ rays—that is to say, according to the observation of basal loops[32–34] for the grains whose basal plane is perpendicular to γ rays. So, for these grains, the direction of the EFG of the iron impurity is parallel to γ rays; in this circumstance, the ratio I_1/I_2 can be smaller than unity, and even reach the limit value 0.33, only if the EFG is positive, while we have noticed it to be normally negative for iron in beryllium.[35] This change of sign when the "anomaly" occurs is well consistent with the disappearance of beryllium atoms to form small dislocation loops on the basal plane around iron impurities. If the minimum possible value for I_1/I_2 is not reached, it means that the recoilless fraction does not completely vanish in the basal plane. This is consistent with typical results obtained from the Mössbauer effect as a technique for measuring diffusion[36]; in the region where diffusion occurs, a fall-off of about 30% or 40% is usually observed in the recoil-free fraction but it does not completely vanish. On the other hand, it is obvious that an anomaly comparable in magnitude to that observed in I_1/I_2 does not occur in the f factor; this result is consistent with the fact that the vibrational contribution of the mean-square displacement decreases while the iron atoms are jumping during the diffusion process.

CONCLUSION

In this investigation, Mössbauer spectroscopy was used to make a contribution to the understanding of iron impurities in beryllium. In particular, the electronic properties of the impurity atom were quantitatively investigated in terms of the existence of a virtual bound state near the Fermi level. It would appear that such studies could be undertaken with other similar matrices, such as cadmium, zinc, or magnesium, showing an axial electric field gradient which may vary with the temperature. On the other hand, it would be interesting to make some macroscopic investigations on the beryllium-iron system, such as heat capacity, electrical resistivity, or magnetic susceptibility, to corroborate the present interpretation of Mössbauer data.

A curious short-range diffusion process of iron atoms with jumps from one site of dislocation loops

to another and subsequent loop annealing seem to be consistent with some anomalous effects which occur in the behavior of the Mössbauer data at about 900 K. However, it may be premature to conclude this definitely, and the point deserves to be made more precise by separating the over-all evolution of the spectra (due to normal behavior of f, ΔS, δ_{iso}, and ΔE_Q) from the perturbations (due to the diffusion process). This can be done by observing all the Mössbauer spectra at the same temperature (such as that of liquid nitrogen) after each controlled annealing of the specimens.

[1]G. K. Wertheim, A. Haussmann, and W. Sander, *The Electronic Structure of Point Defects* (North Holland, Amsterdam, 1971).

[2]C. Janot and G. Le Caer, C. R. Acad. Sci. (Paris) 267, 954 (1968).

[3]R. M. Housley and R. H. Nussbaum, Phys. Rev. 138, 753 (1965).

[4]S. M. Quaim, J. Phys. Chem. 2, 1434 (1969).

[5]F. W. de Wette, Phys. Rev. 123, 203 (1961).

[6]M. Pomerantz and T. P. Das, Phys. Rev. 119, 70 (1960).

[7]W. D. Knight, Phys. Rev. 92, 539 (1953).

[8]R. E. Watson, A. C. Gossard, and Y. Yafet, Phys. Rev. 140, 375 (1965).

[9]R. Ingalls, Phys. Rev. 133, 787 (1964).

[10]A. J. Nozik and M. Kaplan, Phys. Rev. 159, 273 (1967).

[11]B. Baudelet, thesis (University of Nancy, 1970) (unpublished).

[12]S. Yoshida, M. Kiritani, and Y. Shimomura, *Lattice Defects in Quenched Metals* (Academic, New York, 1965), p. 713.

[13]C. Janot and H. Gibert, Mater. Sci. Eng. 10, 23 (1972).

[14]R. M. Housley, J. G. Dasch, and R. H. Nussbaum, Phys. Rev. 136, 464 (1964).

[15]C. Janot and H. Gibert, Philos. Mag. 27, 545 (1973).

[16]*Handbook of Chemistry and Physics*, edited by R. C. Weast (Chemical Rubber, Cleveland, 1972).

[17]A. M. Muir, Report of the Atomic International Division of North American Aviation No. A16695, 1963 (unpublished).

[18]K. A. Gscheider, Solid State Phys. 16, 370 (1964).

[19]J.-P. Schiffer, P. N. Parks, and J. Heberle, Phys. Rev. 133, 1553 (1964).

[20]L. S. Salter, Adv. Phys. 14, 1 (1965).

[21]W. A. Steyert and R. D. Taylor, Phys. Rev. 134, 716 (1964).

[22]C. P. Slichter, *Principles of Magnetic Resonance* (Harper and Row, New York, 1963), p. 174.

[23]P. Jena and T. P. Das, Phys. Rev. 4, 3931 (1971).

[24]P. and R. S. Raghavan, Phys. Rev. Lett. 27, 724 (1971).

[25]C. Kittel, *Quantum Theory of Solids* (Wiley, New York, 1963).

[26]G. Gruner, Solid State Commun. 10, 1039 (1972).

[27]B. Window and G. Longworth, J. Phys. F 1, 718 (1971).

[28]A. P. Klein and A. J. Heeger, Phys. Rev. 114, 458 (1966).

[29]I. Campbell, B. Ferry, P. Imbert, and F. Varret, Saclay Report No. CEA-D.Ph.G/P.S.R.M./826, 1969 (unpublished).

[30]E. Babic, R. Krsnik, B. Leontic, M. Ocko, Z. Vucic, and I. Zoric, Solid State Commun. 10, 691 (1972).

[31]H. D. Pfannes and U. Gonser, Appl. Phys. 1, 93 (1973).

[32]C. Janot and P. Delcroix, Acta Metall. 20, 637 (1972).

[33]R. Le Haziff, G. Donze, J.-M. Dupouy, and Y. Adda, Mem. Sci. Rev. Metall. 61, 467 (1964).

[34]S. Morozomi, T. Furuya, and S. Koda, Trans. Jap. Inst. Met. 11, 127 (1970).

[35]C. Janot, *L'effet Mössbauer et ses applications à la métallurgie physique* (Masson, Paris, 1972).

[36]J. G. Mullen and R. C. Knauer, in *Mössbauer Effect Methodology*, edited by I. Gruverman (Plenum, New York, 1970), Vol. 5, p. 197.